Polymer 49 (2008) 2127–2132

Contents lists available at ScienceDirect

Polymer

journal homepage: www.elsevier.com/locate/polymer

The occurrence of the hexagonal phase in two long chain monodisperse carboxylic acids at high pressure

Ian L. Hosier *

Electronics and Computer Science, University of Southampton, University Road, Highfield, Southampton SO17 1BJ, UK

ARTICLE INFO

Article history:
Received 23 October 2007
Received in revised form 12 January 2008
Accepted 27 January 2008
Available online 4 March 2008

Keywords:
Crystallisation
High pressure
Morphology

ABSTRACT

High-pressure differential thermal analysis (DTA) experiments have allowed the pressure–temperature phase diagrams to be constructed for the monoacid CH_3–$(CH_2)_{190}$–COOH and the diacid HOOC–$(CH_2)_{192}$–COOH. The current work follows on from previous work concerning the high-pressure phase of various monodisperse *n*-alkanes. The use of a diamond anvil cell calibrated from DTA data has allowed the morphology of each sample to be investigated as a function of pressure and temperature and for the crystallization, melting and hexagonal/orthorhombic transitions to be examined directly. It was shown that the monoacid displayed a similar behaviour to the *n*-alkane of twice its chain length due to end group pairing, whereas the diacid shows a wider hexagonal stable region, which extends to pressures as low as 0.35 GPa. This enhanced stability is thought to be due to increased configurational entropy due to unlimited end group association.

1. Introduction

The high-pressure phase of polyethylene discovered in 1974 [1] had been predicted two years earlier, from thermodynamic data, by Bassett and Turner [2,3] who proposed that its crystallization from the melt was responsible for the associated large lamellar thicknesses reported by Geil et al. [4] in 1964. It was shown [5,6] that formation of the familiar orthorhombic phase gave way to a new process, with a discontinuity of supercooling (for crystallization on cooling at ~1 K/min) from greater than or equal to ~15 K to ~12 K and a change in morphology from a spherulitic to a distinctive coarse sheaflike, spiky texture. These two characteristic textures were subsequently confirmed [1] to be the products of two distinct processes of crystallization from the melt, i.e. of the orthorhombic and hexagonal phases, respectively. The supercoolings cited [3] imply, moreover, that crystallization of the hexagonal phase at these rates practically always occurs in the orthorhombic-stable region – the exception being for very long molecules at the lowest supercooling. The large lamellar thicknesses formed in the hexagonal phase, with its low entropy of fusion, are transferred to the orthorhombic phase during the return to ambient conditions. This first-order transition brings about tilting of molecules, which is normal to the lamellar surfaces in the hexagonal phase [1], but is inclined at 35° to the lamellar normals in the orthorhombic phase [7] corresponding to fold surfaces of approximately {201} planes.

The phase diagram constructed by Bassett and Turner [2,3] showed that the area of stability for the hexagonal phase widens with pressure. The stability range of the hexagonal or rotator phases of the short *n*-alkanes, on the other hand, decreases and disappears with increasing pressure [8,9]. This dichotomy corresponds, in thermodynamic terms, to the difference between phases of high entropy and high volume, inviting the question of what molecular length is required to effect the change.

High-pressure DTA (differential thermal analysis) measurements showed [10] that the isobaric stability range decreased for shorter molecules to ~10^4 in molecular weight. Moreover, solvent extraction of the lower end of the molecular distribution from commercial polyethylenes avoided segregation of low melting populations on crystallization at ~0.5 GPa which was a major cause of brittleness [11]. Molecular length measurements, by GPC, of such populations after selective extraction, gave ~60 nm average chain length ($M_w(C_{475}H_{952})$ ~ 6600 g/mol) as the lower limit to enter the high-pressure phase [12]. In a more detailed study, Asahi found [13] that fractions of 1000 and 2000 molecular weight did not show the high-pressure phase to ~1 GPa but those of 6500 and above did. However, the development of the hexagonal phase in *n*-alkanes of lesser molecular weight (~3500 g/mol) was confirmed recently [14]. The morphologies and phase diagrams of the three *n*-alkanes $C_{390}H_{782}$, $C_{294}H_{590}$ and $C_{246}H_{494}$ were successfully established using a DTA technique where the melting point was used as a calibration of cell pressure in diamond anvil experiments. Use of a diamond anvil cell allows the morphology and any high-pressure transitions to be examined directly, a feature not available with conventional DTA. In the two longer *n*-alkanes, high-pressure

* Tel.: +44 (0) 23 8059 3429; fax: +44 (0) 23 8059 3709.
E-mail address: ilh@ecs.soton.ac.uk

0032-3861/$ – see front matter © 2008 Elsevier Ltd. All rights reserved.
doi:10.1016/j.polymer.2008.01.074

phases were observed at pressures exceeding ~0.6 GPa but in the shorter *n*-alkane, only at pressures exceeding ~0.9 GPa. At lower pressures, hexagonal crystals form only on crystallization in a metastable state, at still lower pressures, only orthorhombic crystals formed. So far as we are aware, n-$C_{246}H_{494}$ is the shortest *n*-alkane in which the high-pressure hexagonal phase has so far been reported. Increasing length favours formation of the high-pressure phase because of the increased entropy it brings, presumably from configurational disorder along the chain.

In addition Asahi [13] reported a solid/solid phase transition (to a hexagonal phase) at 0.58 GPa and 201 °C in 1,20 eicosanoic acid, HOOC–$(CH_2)_{18}$–COOH ($M_w = 342$ g/mol) which was attributed to association of the acidic end groups. The resulting reduction in the entropy of the melt, raises its free energy and hence increases the melting points of the resulting crystal phase [2,3]. So far this is the lowest molecular weight organic compound in which the hexagonal phase has been reported. We now report on complementary observations of a high-pressure phase in two other carboxylic acids; the monoacid CH_3–$(CH_2)_{190}$–COOH and the diacid HOOC–$(CH_2)_{192}$–COOH.

2. Experimental

2.1. Nomenclature

The monoacid CH_3–$(CH_2)_{190}$–COOH and the diacid HOOC–$(CH_2)_{192}$–COOH were synthesized by Dr. G.M. Brooke and colleagues at the University of Durham, following Whiting [15,16], under the auspices of EPSRC. For convenience these will be denoted by MA1 and DA1, respectively. The monodispersity of both materials was checked by mass spectroscopy and no detectable impurities were found in either case.

2.2. High-pressure DTA procedure

High-pressure differential thermal analysis (DTA) experiments were carried out using an oil filled piston cylinder press as previously [14,17]. Samples of the required material and a PTFE reference (each ~10 mg) were wrapped in aluminium foil prior to insertion into the DTA cell. The temperature scale was calibrated against the melting of high purity indium as standard. DTA heating scans were then performed at constant pressure in the range 0.1–0.8 GPa with scan rates ranging from 2 K/min at the lowest temperatures to 0.5 K/min at the highest temperatures, these being limited by the thermal mass of the press and heat losses. The DTA signal was amplified by a Linear Technology LT1050 chopper stabilised amplifier with low pass filtering before being fed to a Keithley Model 181 Nanovoltmeter. Simultaneously the sample temperature was monitored on an electronic thermocouple display (accuracy ±1 K). The DTA signal plotted against temperature allowed the endothermic transitions to be determined reproducibly. The melting temperatures at a variety of different pressures were then used to calibrate the pressure obtained in a diamond anvil cell (DAC).

2.3. Diamond anvil cell (DAC) procedure

Samples were placed into a 0.6 mm diameter hole bored in a 50 μm thick sheet of nickel alloy and were melted gently on a Kofler WME hot-bench so as to form a continuous film inside the hole. The sheet with sample was then inserted between parallel diamonds of a gasketed Diamond Anvil Cell, constructed to the design of Barnett et al. [18] and fitted with an external heater, similar to that on which the high-pressure phase was first discovered [1]. With the hole centred optically, a moderate pressure was applied, at ambient temperature, so as to hold the sample tightly in place and the entire assembly was then mounted on the stage of a Vickers universal polarizing microscope, allowing the crystallization process to be observed *in situ* and photographed through the diamonds.

Experiments were performed at pressures for which the melting point of the sample was between 190 and 290 °C. Temperatures higher than this were not used due to concerns of possible degradation and crosslinking, for pressures much less than that required to give a melting point of 190 °C the sealing of the gasket was poor resulting in leakage of the contents. To set a desired pressure in the DAC the specimen was first melted at 145 °C and then the pressure was increased slightly to induce immediate recrystallization and prevent leakage. The melting temperature at the new pressure was then determined; this was compared to the required melting temperature (obtained from the DTA calibration procedure) and the load was adjusted accordingly.

Having obtained the required melting point the proper experiment was then performed at constant pressure,[1] the temperature was raised 10 K above the initial melting temperature (T_I) to melt the specimen completely. The temperature was then reduced to 15 K below T_I to induce crystallization and, when the morphological changes were complete, a photograph was recorded. The temperature was then reduced in 10 K steps to 150 °C and a photograph of the cell morphology was recorded at each step. An equivalent procedure was then adopted on reheating the cell contents. For a run to be acceptable the final melting point (T_F) had to be the same as T_I since any change indicated leakage of the cell contents and subsequent loss of pressure.

For each experiment a fresh sample was prepared in a fresh gasket and the diamonds were scrupulously cleaned to avoid cross-contamination of these ultra pure materials. The scale of the microscope was calibrated using a standard graticule at room temperature.

2.4. Stability of the hexagonal phase

Although it is normal for the hexagonal phase to crystallize in a metastable condition at finite supercoolings [3], its thermodynamic stability in relation to the phase diagram can be assessed on re-melting. There is little or no superheating on melting because of the presence of suitable nuclei so that the presence or absence of the two successive first-order transitions from orthorhombic to hexagonal to melt in the DTA indicates whether the hexagonal phase is, or is not, stable under the operating pressure. In the diamond anvil cell an equivalent test is reproduction of the original hexagonal texture on reheating the specimen. If the original texture is reproduced on heating then the hexagonal phase is said to be stable (at that pressure), but if the hexagonal phase is not reproduced then it is said to be metastable.

3. Results

3.1. Phase behaviour

DTA experiments allowed the phase diagrams of the two samples to be obtained as a function of pressure. Fig. 1 shows an example of the raw DTA data obtained from DA1, at 0.23, 0.46 and 0.77 GPa. At 0.23 GPa the DTA peak is singular indicating the presence of the orthorhombic phase, whereas at pressures of >0.4 GPa two peaks were detected indicating in turn; the orthorhombic to hexagonal transition and finally the melting of the hexagonal phase [8]. Similar DTA measurements over a range of different pressures allowed the phase diagrams for both materials to be constructed

[1] Strictly the DAC works under constant volume and not constant pressure, therefore, values of nominal cell pressure are quoted.

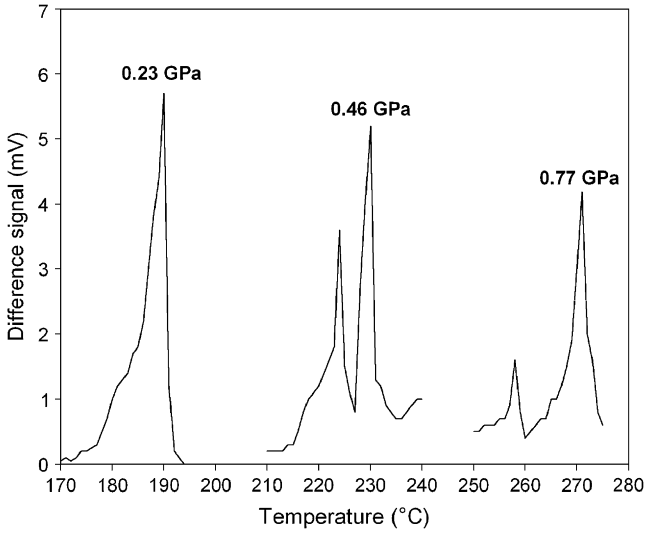

Fig. 1. Raw data from the DTA experiments for DA1 crystallized at the indicated pressures.

and these are shown in Fig. 2a and b for MA1 and DA1, respectively. Where two DTA melting peaks occur, the lower phase line is constructed using the temperature corresponding to the maximum value of the lower DTA peak and the upper phase line is constructed using the temperature corresponding to the maximum value of the upper DTA peak. This process allows the phase diagrams to be constructed with a typical uncertainty of ±5 °C and ±0.01 GPa within the range of the data, and with a greater uncertainty on extrapolation to higher pressures as shown by the dotted lines (quadratic fit). The upper (melting) phase line then allows, for each material, the nominal cell pressure to be determined in the DAC by measuring (optically) the melting of the contents. Clearly, from Fig. 2, the region of stability is less for MA1 than for DA1 as expected [13] due to the association of acidic end groups.

The comparable results from the DAC experiments are summarised in Table 1; this table indicates the temperatures at which the contents of the cell melt at the start (T_I) and end of the experiment (T_F), the value for T_I was then used to calculate the nominal cell pressure (P_{NOM}) using the phase diagrams of Fig. 2. One of three behaviours was exhibited depending on the sample and pressure

Table 1
DAC results from MA1 and DA1 crystallized at the indicated pressure

Material	P_{NOM} (GPa)	T_I (°C)	T_F (°C)	Phase	T_1 (°C)	T_2 (°C)
MA1	0.32 ± 0.01	205	210	O	–	–
	0.50 ± 0.01	230	240	M	210	190
	0.54 ± 0.01	235	240	M	210	190
	0.64 ± 0.01	250	250	H	230	200
	0.77 ± 0.01	260	270	H	240	210
	1.0 ± 0.05	280	275	H	250	210
	1.0 ± 0.05	280	285	H	250	210
	0.9 ± 0.06	270	275	H	250	220
DA1	0.27 ± 0.01	200	200	M	180	160
	0.33 ± 0.01	210	220	M	190	170
	0.39 ± 0.01	220	220	H	200	180
	0.58 ± 0.01	250	255	H	220	200
	0.58 ± 0.01	250	270	H	230	200
	0.65 ± 0.01	260	265	H	230	210
	1.0 ± 0.05	280	280	H	250	210

which are denoted by O, M or H in the table. O implies that orthorhombic crystals are formed at all temperatures, M is when the hexagonal phase crystallised in the metastable phase but did not reform on reheating; H indicates that the hexagonal phase is stable occurring between the orthorhombic and melt phases during both the crystallisation and melting sequences. Where hexagonal crystals do form, further cooling causes them to convert to the orthorhombic phase evidenced by a change in the birefringence beginning at temperature T_1 and completing at temperature T_2. Table 1 indicates, as expected, that these temperatures lie close to the lower phase lines plotted in Fig. 2. In particular, the hexagonal phase was not detected in MA1 below ~0.5 GPa whereas this phase was stable in DA1 at pressures ~0.4 GPa. This confirms the above DTA results and those of Asahi [13].

3.2. Morphology of the monoacid (MA1)

The pressure of 1 GPa was taken to illustrate the typical behaviour of this monoacid, which follows closely the behaviour of C390 [14].

Fig. 3a shows crystals obtained from the melt at 270 °C, these are the distinctive needle like crystals expected from crystallization in the hexagonal phase [1,14,17]. At 250 °C, (Fig. 3b) space is filled and the crystals are still quite distinct, at 240 °C the conversion to the orthorhombic phase has begun and interpretation becomes more

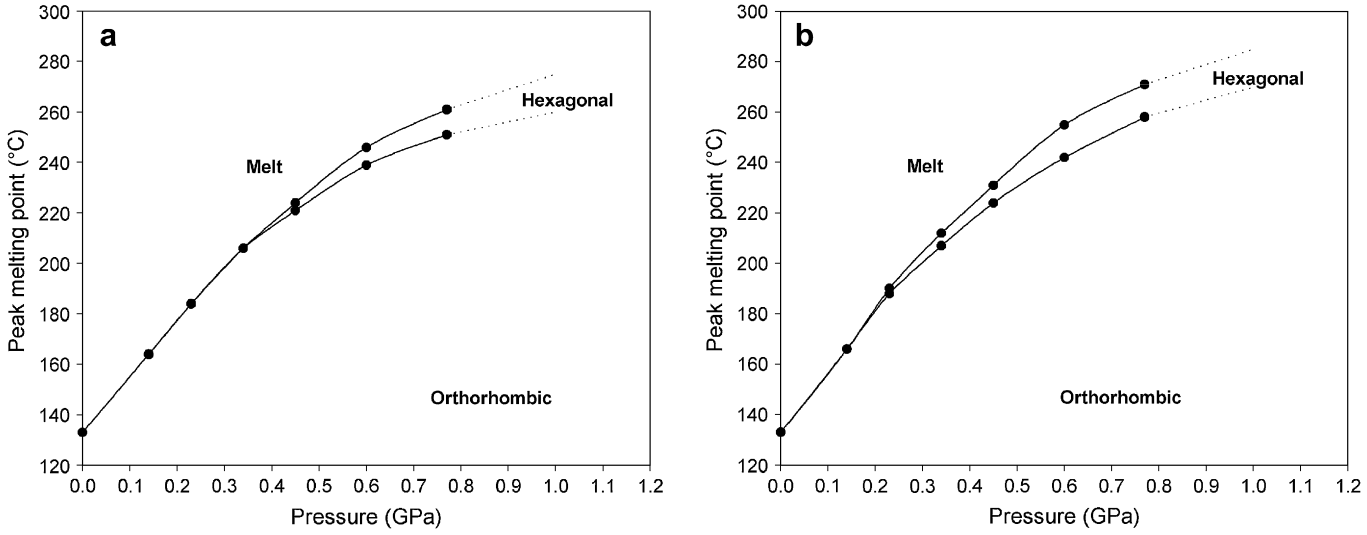

Fig. 2. Phase diagrams obtained from the DTA experiments for (a) MA1 and (b) DA1.

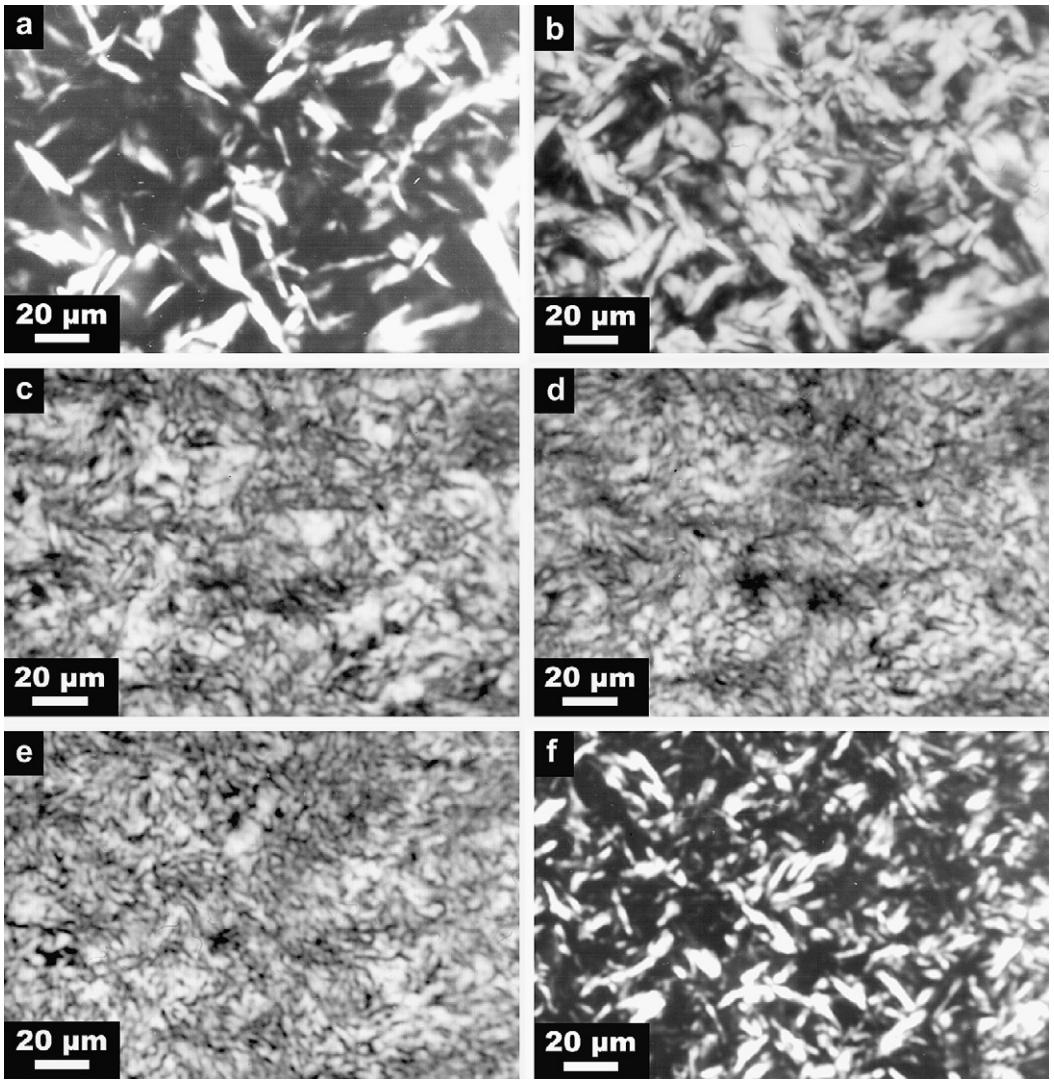

Fig. 3. Monoacid MA1 crystallized at 1 GPa: (a) 270 °C, (b) 250 °C, (c) 240 °C, (d) 230 °C, (e) 150 °C and (f) reheated to 265 °C.

difficult (Fig. 3c), however, the features in Fig. 3b are largely preserved. Below ~230 °C, the morphology becomes finer in nature and the detail of individual crystals is completely lost; the texture at 230 °C (Fig. 3d) is similar to that at 150 °C (Fig. 3e) and is clearly orthorhombic. Finally, on reheating to 270 °C (Fig. 3f) some memory of the original hexagonal crystal texture is retained but the reconverted crystals appear more ragged and disjointed in appearance, mainly because of the rapid onset of melting following the conversion.

3.3. Morphology of the diacid (DA1)

Unusually the diacid DA1 was the only material so far considered that is capable of exhibiting metastable hexagonal crystals at the unusually low pressure of 0.27 GPa. An example of these crystals is shown in Fig. 4a, on further cooling these crystals readily transform to an orthorhombic phase (Fig. 4b), which on subsequent heating melts directly, indicating that the crystals are metastable at this pressure.

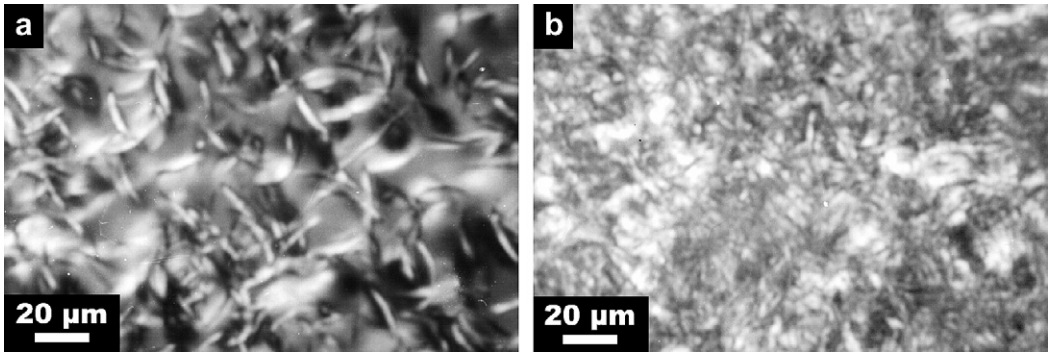

Fig. 4. Diacid DA1 crystallized at 0.27 GPa: (a) 190 °C and (b) 170 °C.

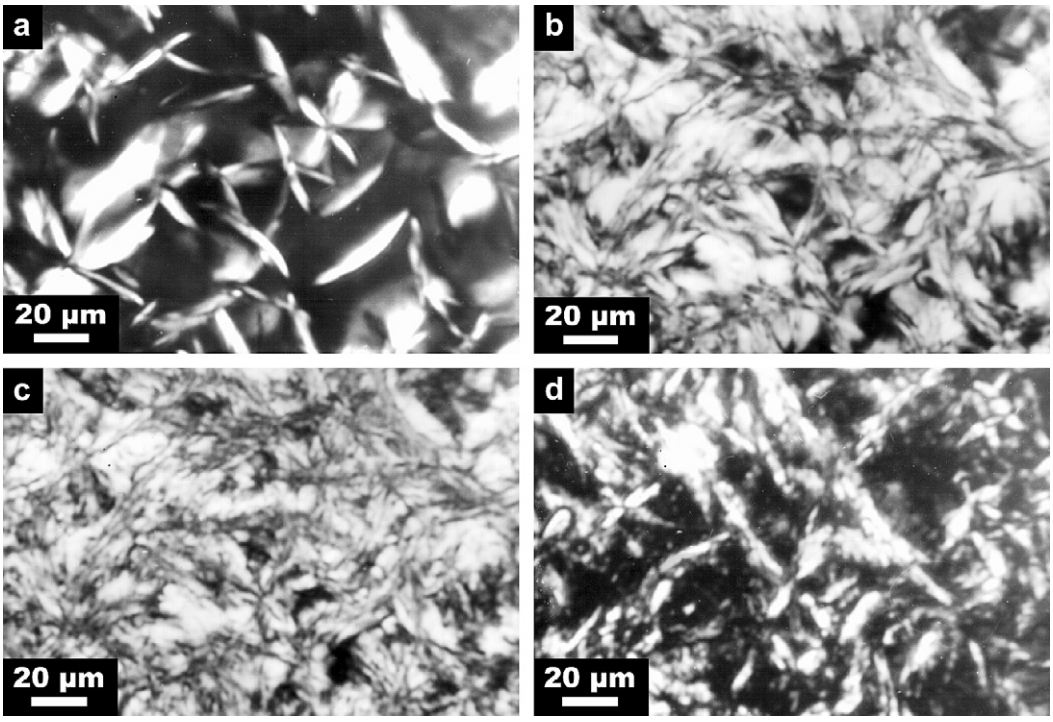

Fig. 5. Diacid DA1 crystallized at 0.65 GPa: (a) 250 °C, (b) 230 °C, (c) 210 °C and (d) reheated to 270 °C.

When crystallized at 260 °C and 0.65 GPa stable hexagonal crystals readily form (Fig. 5a), transformation of these crystals only begins at 230 °C (Fig. 5b), indicating an unusual longevity, where they are rapidly converted into the orthorhombic phase (Fig. 5c). On reheating, memory is retained of the original texture (Fig. 5d), however, the crystals look ragged and indistinct due to the onset of melting which rapidly follows the re-conversion.

4. Discussion

In order for the hexagonal phase to form at all during crystallization, the temperature and pressure must be such that the crystallization occurs in the hexagonal region of the phase diagram. On lowering the temperature, the crystals transform to the orthorhombic phase on crossing the lower phase boundary. On reheating, the reverse transformation occurs if the width of the hexagonal stable region is wide enough. For instance in DA1, at 0.65 GPa, the width of this region is only some 10 K or so and so is close to the temperature step used in the experiments, for this reason only a partial transformation (Fig. 5d) is observed in the DAC prior to melting.

Thus the DAC data are in general agreement with the phase diagrams as determined by high-pressure DTA. In the former, the transitions are broadened by changes in pressure during transformations, (since the DAC operates in a constant volume, not constant pressure, mode) – the parameter T_2 in Table 1 reflects this broadening, the relevant transition occurs over some 20–30 K or so in the DAC but the corresponding DTA peaks are quite sharp.

The carboxylic acids are known, from the example of 1,20 eicosanoic acid, to form a high-pressure hexagonal phase for very short molecules, which can, however, form long associations by pairing their acidic end groups through hydrogen bonding [13]. A fall in the entropy of the melt seems the most likely explanation for the phenomenon: any such pairing will reduce the number of ways molecules can organize in the melt. However, whereas diacids may associate indefinitely, this is not the case for the monoacids, which are limited to pairing. For CH_3–$(CH_2)_{190}$–COOH (MA1), the bimolecular length is approximately that of $C_{390}H_{782}$ (the longest *n*-alkane studied) so that it is no surprise that it, too, should form a high-pressure phase and displays a nearly identical phase behaviour to this *n*-alkane [14]. Indefinite association is strikingly demonstrated here by the formation of a metastable hexagonal phase in the diacid HOOC–$(CH_2)_{192}$–COOH (DA1) at the unusually low pressure of 0.27 GPa, a pressure, at which even in regular polyethylene [2,3], a hexagonal phase is never observed.

5. Conclusions

In agreement with previous studies on the monodisperse *n*-alkanes, the monodisperse carboxylic acids CH_3–$(CH_2)_{190}$–COOH and HOOC–$(CH_2)_{192}$–COOH also form stable high-pressure phases at pressures similar to those used to induce the hexagonal phase in *n*-alkanes of twice their chain length. This is thought to be due to pairing of their acidic end groups. However, the diacid showed a significantly wider hexagonal stable region than the monoacid or any of the previously investigated *n*-alkanes and this is thought to be due to unlimited end group association.

Acknowledgements

The work described herein was carried out at the Department of Physics at the University of Reading with the kind permission of Prof. David Bassett. We would also like to thank Mr. C.J. Balagué for his valuable assistance with the experiments performed on the high-pressure piston cylinder press. The work was supported by EPSRC under whose auspices the monodisperse acids used were prepared, characterised and supplied by Dr. G.M. Brooke and colleagues at the University of Durham.

References

[1] Bassett DC, Block S, Piermarini GJ. J Appl Phys 1974;45(10):4146–50.
[2] Bassett DC, Turner B. Nat Phys Sci 1972;240(103):146–8.
[3] Bassett DC, Turner B. Philos Mag 1974;29(4):925–55.
[4] Geil PH, Anderson FR, Wunderlich B, Arakawa T. J Polym Sci Part A Polym Chem 1964;2:3707–20.

[5] Bassett DC, Khalifa BA, Turner B. Nat Phys Sci 1972;239(94):106–8.
[6] Bassett DC, Turner B. Philos Mag 1974;29(2):285–307.
[7] Bassett DC. Principles of polymer morphology. Cambridge: Cambridge University Press; 1981. p. 170.
[8] Nelson RR, Webb W, Dixon JA. J Chem Phys 1960;33(6):1756–64.
[9] Wurflinger A, Schneide GM. Ber Bunsenges Phys Chem 1973;77(2):121–8.
[10] Bassett DC. Polymer 1976;17(6):460–70.
[11] Bassett DC, Carder DR. Philos Mag 1973;28(3):513–33.
[12] Olley RH. Unpublished data.
[13] Asahi T. J Polym Sci Polym Phys Ed 1984;22(2):175–82.
[14] Hosier IL, Bassett DC. Polymer 2002;43(22):5979–84.
[15] Paynter OI, Simmonds DJ, Whiting MC. J Chem Soc Chem Commun 1982;20:1165–6.
[16] Bidd I, Holdup DW, Whiting MC. J Chem Soc Perkin Trans 1 1987;(11):2455–63.
[17] Vaughan AS, Ungar G, Bassett DC, Keller A. Polymer 1985;26(5):726–32.
[18] Barnett JD, Piermarini GJ, Block S. Rev Sci Instrum 1973;44(1):1–9.